



Analysis of the Reserve of Iron Ore using the Cellular Neural Networks (CNN) Method

Ali Muhittin Albora

Istanbul University-Cerrahpaşa, Engineering Faculty, Geophysical Department, 34850, Büyükçekmece-Istanbul, Turkey

Email: muhittin@istanbul.edu.tr

Abstract As is known, the separation of regional and residual areas is an important issue in gravity and magnetic prospection methods. The aim is to determine the real structures and properties of the objects at the depth of study with the least error. In this study, with the CNN method, we can purify the structures at the desired depth from noise and view the residual structures. Here, the magnetic anomaly map obtained from the magnetic study of the Bingöl region Heylantepe location right above the iron deposit was distinguished by using the CNN method and the Residual anomaly map was obtained. The underground iron ore was modeled from the section taken from the residual anomaly map.

Keywords Cellular Neural Networks (CNN) Method

Introduction

Cellular Neural Networks (CNN), a special type of artificial neural networks, was first introduced in 1988 by Leon Chua and Lin Yang. They are dynamic artificial neural networks that are interconnected and composed mostly of two-dimensional cells. The most important feature that distinguishes CNN from artificial neural networks as we know it is that the link weight coefficients form an invariable link network on the plane of study. This puts CNN in a very advantageous position compared to artificial neural networks in the classical sense. In addition to having some basic features of the known artificial neural networks, they find quite a lot of application areas in image processing and image recognition, especially because of their two-dimensional structures [1-5]. In this study, the Cellular Artificial Neural Network (CNN) method, which is frequently used in image processing today, was applied to the Magnetic anomaly map obtained from the region as a discrimination method, and a very good result was obtained compared to classical methods. A good result was obtained when the residual map found was correlated with the drillings. Some researchers such as [6-10] have made important studies on CNN.

Methods

Cellular Artificial Neural Networks are mostly structures made up of cells arranged to form a two-dimensional array. CNN is a method that allows to reveal certain properties of two-dimensional images, requires preliminary training and is quite frequently used in image processing. Unlike the known artificial neural networks, every cell here is in contact with the cells in its immediate neighborhood (Figure-1).



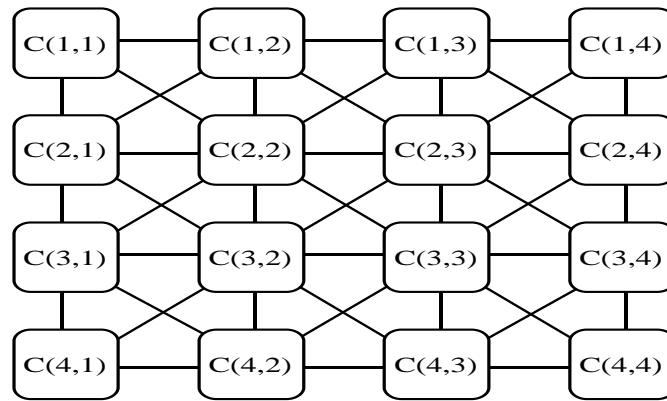


Figure 1: Two Dimensional (4x4) Cellular Artificial Neural Network [9]

Each cell in these structures:

- a) A linear input unit with weighted addition
- b) A linear dynamic interface
- c) It is a dynamic circuit consisting of a piece-wise linear (pwl) output unit symmetrical with respect to the n-piece (generally three-piece) origin (Figure-2).

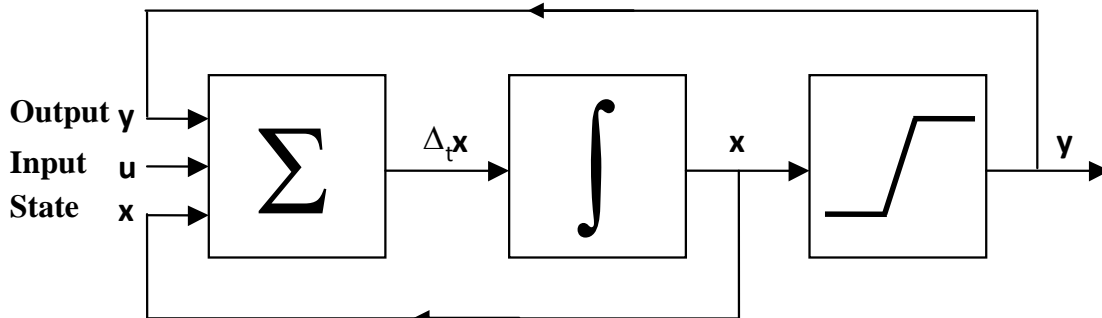


Figure 2. Block Diagram of an Artificial Neural Network [9].

The r-neighborhood of a cell in the Cellular Artificial Neural Network (CNN) is defined as follows.

$$N_r(i, j) = \{C(k, l) | \max(|i - k|, |j - l|) \leq r, \quad 1 \leq i \leq M; 1 \leq j \leq N \} \tag{1}$$

(i, j) : The index vector that determines the location of the cells in the array,

$C(i, j)$: I. Row is the parameter that indicates the location of the cell in the J. column.

The differential equations that characterize the Cellular Artificial Neural Network can be written as:

$$\frac{dx_{i,j}(t)}{dt} = -S \cdot x_{i,j}(t) + \sum_{(k,l) \in N(i,j)} A_{i,j;k,l} \cdot y_{k,l}(t) + \sum_{(k,l) \in N(i,j)} B_{i,j;k,l} \cdot u_{k,l}(t) + I_{i,j} \tag{2}$$

$$y_{i,j}(t) = f[x_{i,j}(t)] = \frac{1}{2} \cdot (|x_{i,j}(t) + 1| - |x_{i,j}(t) - 1|) \tag{3}$$

here :

$A_{i,j}$: feedback link weight coefficients

$B_{i,j}$: input connection weight coefficients

I: threshold level, which is generally the same for every cell

S: state feedback is defined as the weight coefficient.



The equation that characterizes the Discrete Time Cellular Artificial Neural Network is expressed as follows.

$$x_{i,j}(n+1) = \sum_{(k,l) \in N(i,j)} A_{i,j;k,l} \cdot y_{k,l}(n) + \sum_{(k,l) \in N(i,j)} B_{i,j;k,l} \cdot u_{k,l}(n) + I_{i,j} \tag{4}$$

$$y_{i,j}(n) = f[x_{i,j}(n)] = \frac{1}{2} \cdot (|x_{i,j}(n) + 1| - |x_{i,j}(n) - 1|) \tag{5}$$

If it is considered in this equation, besides the classical filtering, an iterative filtering from the feedback link weight coefficients a is also performed. Here, the entries of the cells are real numbers that take values in the range of $u_{i,j}$, [-1,1]. the outputs of the cells are y_i and j are outputs that can only take -1 or +1 values if the stability conditions are met at the end of a certain period (or cycle). One of the most important features that distinguishes CNN from known artificial neural networks is that the feedback (a) and input (b) connection weight coefficients form an invariable connection network on the working plane (space invariance property) (Figure-3).

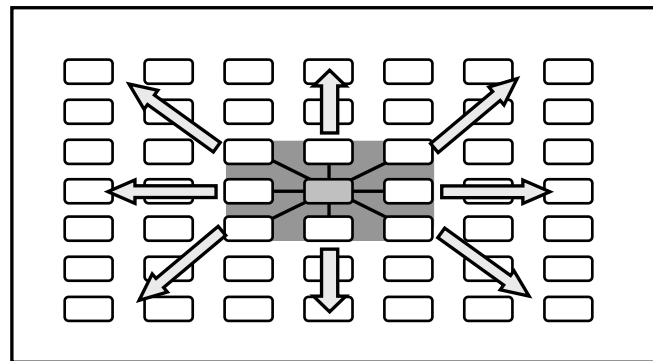


Figure 3: The invariance property in the plane [9]

$$A(i, j; k, l) = A(k - i, l - j) \quad B(i, j; k, l) = B(k - i, l - j) \tag{6}$$

Application of Nomograms to Synthetic Data

CNN has been applied in geophysical methods in regional and residual separation of magnetic anomaly maps from potential field sources. In Table 1, 3 prisms with different depths, coordinates, Inclination, Declination, and Susceptibility are given with different angles with the Magnetic North. Where X1, X2 are the distance of the starting and ending points on the X axis from the origin of the prism; Y1, Y2 is the distance of the starting and ending points on the Y axis from the origin of the prism. The upper surface depth of the prism is h1, the lower surface depth of the prism is h2, the inclination angle is I, the equation angle is D, the angle of the prism with the magnetic north, and the susceptibility is k. The Total magnetic anomaly map created by prisms with different parameters given in Table 1 is shown in Figure 4. The map obtained after applying CNN to this magnetic anomaly map is given in Figure 5. As can be seen in this map, a good distinction is made, revealing two prismatic structures close to the surface and reducing the effect of the prism, which is relatively deeper and has a strong effect [10].

Table 1: Total magnetic field parameters consisting of 3 prisms, (Total area (F) = 46000 gamma, Inclination = 67, Equation = 25) [10].

Pr	X ₁	X ₂	Y ₁	Y ₂	h ₁	h ₂	I	D	β	k
1	20	25	30	35	5	8	67	20	0	0.00193
2	32	36	17	21	4	6	66	24	5	0.00198
3	22	32	22	26	8	13	65	25	4	0.00205

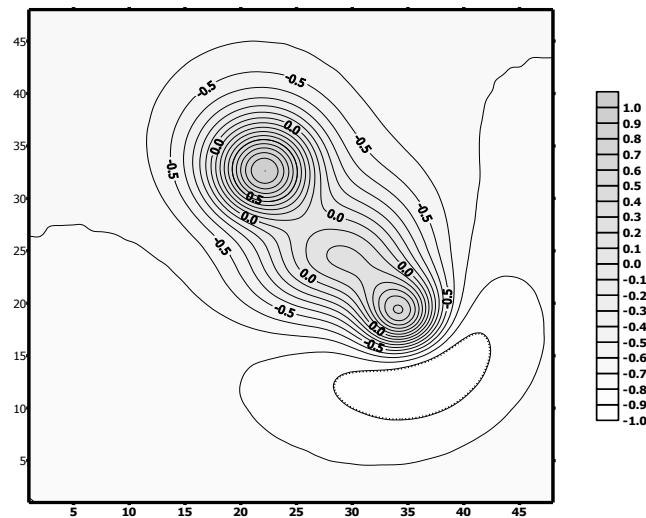


Figure 4: Total magnetic field anomaly map consisting of 3 prisms [10]

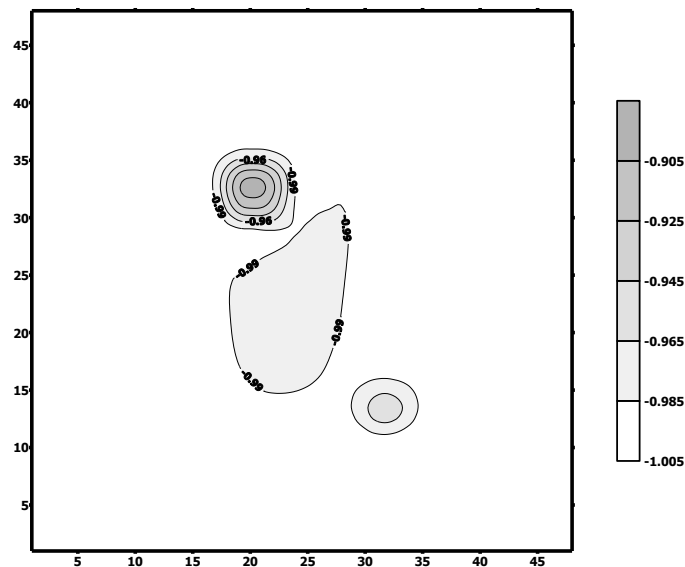


Figure 5: CNN output of the total magnetic anomaly map (contour interval is taken as 0.02nT) [10]

CNN Bingöl Region Land Application

In the field study, magnetic anomaly map prepared by MTA to search for iron mines in Bingöl region was used. The place where the mine field in Bingöl region is located is mentioned as Avnik location. Figure 6 shows the geological map of the Bingöl iron ore. In this study, only the Haylandere bed part of the Avnik locality, which is quite wide, has been considered (Figure 7). Avnik iron deposits are massive and lenticular in shape and consist mainly of magnetite and a small proportion of apatite and amphibole minerals [11]. The ore type in the form of scattered magnetite zones is encountered in speckled amphibolites and metavolcanites.

The most economically important deposits of the study area are located in the transition zone of the gneiss unit and the felsic metatuff-metavolcanic unit and along the section where the rocks of both units alternate [11]. The deposits in the Avnik region have almost the same stratigraphic features as stratigraphically. The beds in the Haylandere area are not linked to other deposits. The northern part of the deposit is covered with alluvium and the ore body is surrounded by the Avnik granitoid, the side rocks are gneiss and amphibolites cut and assimilated by the granite [11]. Massive iron ore lenses are NW-SW and OD inclined; Massive, banded and



sparsely scattered iron ore is present in the bed and is concentrated especially around the H9 drilling. Also Haylanderesi deposit is connected to the Gönaçtepe deposit by small lenses [11].

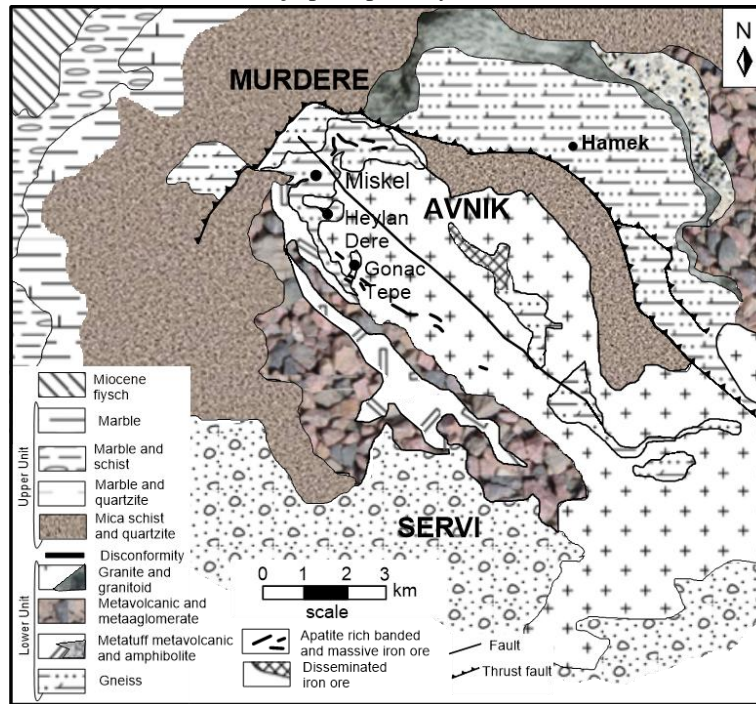


Figure 6: The geology and inventions map of Bingöl iron ore (Avnik region) has been modified from [12]

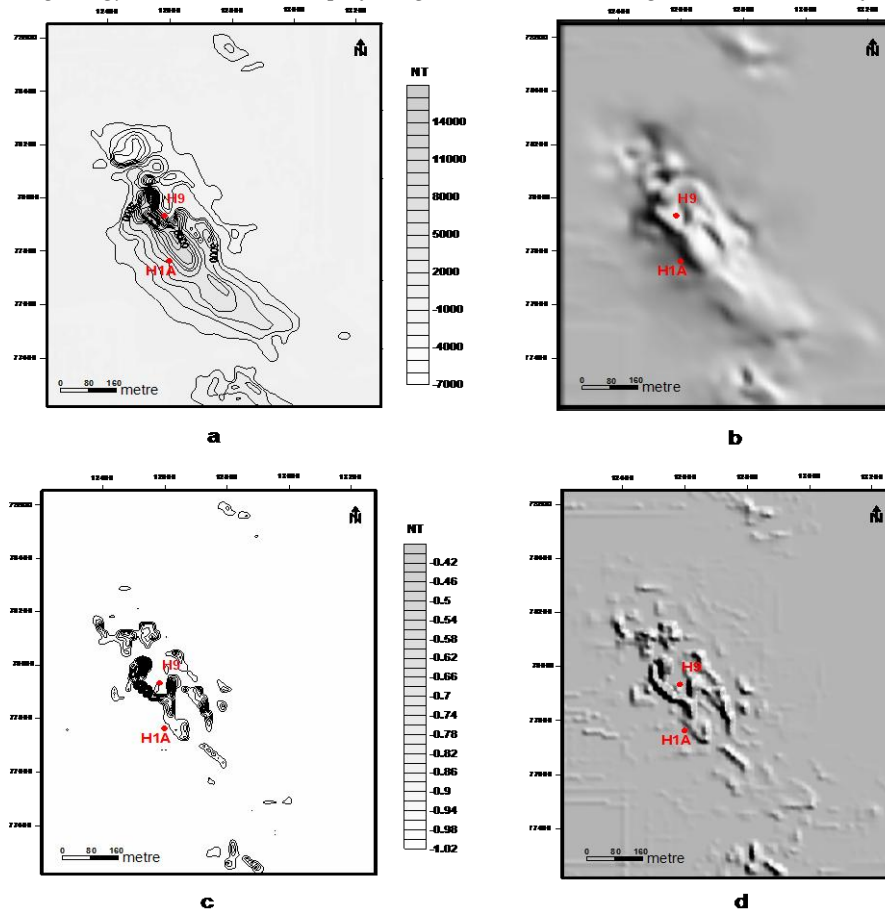


Figure 7: a) Magnetic anomaly map of Heylandere location in Bingöl region. b) Relief printout of the magnetic anomaly map. c) CNN printout of the magnetic anomaly map. d) Relief map of the CNN output

When the Heylandere deposit is examined (Figure 7a), it is seen that mostly magnetic anomaly maps are collected in one region. The values of the magnetic anomaly map range from -7000nT to 14000nT. In Figure 7b, the relief printout of the magnetic anomaly map is given. Figure 7c shows the Cellular Artificial Neural Network output of the magnetic anomaly map. Here, the coefficient A is taken as 0. In Figure 7d, the relief printout of this map is given.

When the Cellular Artificial Neural Network output is examined, it is seen that anomalies are quite strong. H1A and H9 drillings have been made close to the anomalies, and the mine is mostly observed where H9 drilling is available. As seen in Figure 8, there are 2 (H1A, H9) drillings in this area. The purpose of these drillings in areas with low anomaly values is to determine whether there is ore presence in deeper regions. As can be understood from the drill steep sections, the ore is quite deep, so it does not have an economic feature.

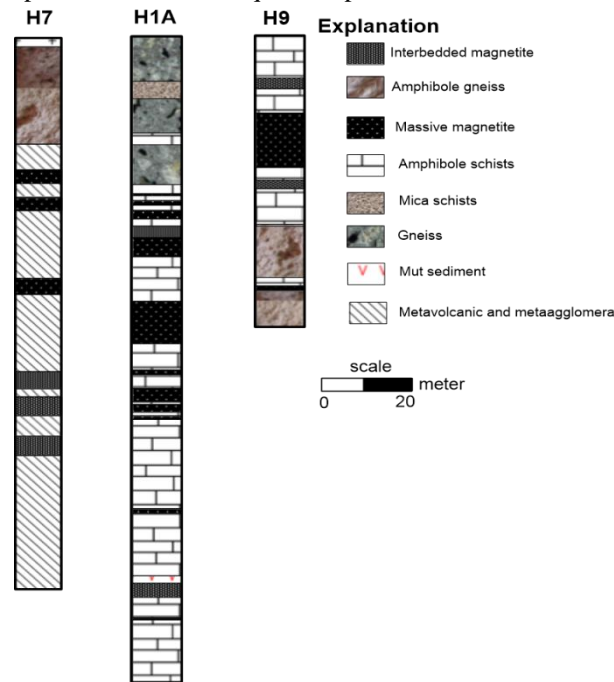


Figure 8: Drilling strut sections of Heylandere location (H1A, H7, H9) and Lagand

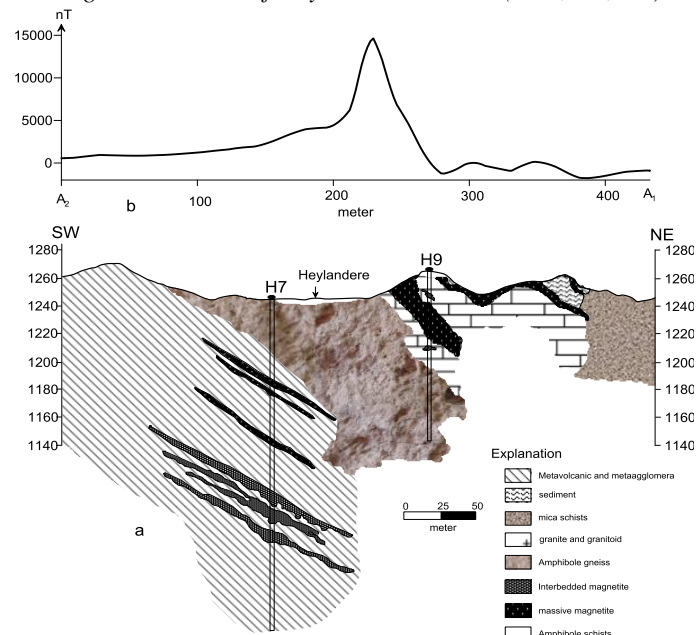


Figure 9: a) Geological section of the region where the ore is located b) B1 - B2 cross section magnetic anomaly of the region

Results

It is very important to use the CNN method especially in residual anomaly separations. It is clear that CNN gives good results from many known classical methods. There is no data loss because CNN evaluates according to the neighborhood relationship according to classical methods. It also finds uses as a CNN boundary detection method. As the CNN limit detection method, it gives more successful results than classical methods. For this reason, CNN has been used frequently in geophysical methods lately. In this study, CNN was applied to the iron ore in Bingöl region Heylandere location and regional and residual separation was made. When we look at the occlusions in the residual anomaly map given in Figure 7, we see that iron ore concentrates in these regions. Here, we compared the CNN output we obtained with the information obtained from the drillings made by the Mineral Technical Exploration Institute (MTA) in this region. As can be seen in the boring log given in Figure 8, the H1A drilling was made outside of the anomaly effect and massive magnet was cut at depth as seen in the drilling section. When the H9 sounding is examined, the massive magnet is closer to the surface and it is located where there is a strong anomaly effect. As a result, it has been observed that the CNN output given in Figure 7c has a good fit according to the H9 drilling data. In the region called Avnik region, good results were obtained from the magnetic methods in the geophysical studies carried out in Heylandere, Gonanç hill, Kelme hill and Kihlaz regions, and drilling studies were carried out in regions where anomalies are intense. From the residual anomaly maps obtained using CNN after magnetic studies, very strong anomaly values were obtained at the locations of the mine. A geological section was prepared using the borehole data obtained in the study conducted by [11] in the Heylandere region (Figure 8). The underground course of the mine, which is exposed on the surface, was understood from the magnetic anomaly map and H9 drilling was made. In the area of H9 drilling, a mine was cut at a certain depth.

Reference

- [1]. Suzuki, H., Matsimoto T. and Chua L.O., "A CNN Handwritten Character Recognizer", *International Journal of Circuit Theory and Applications*, 20: 601-612, 1992.
- [2]. Matsumoto T., Chua L.O. and Yokohama T., "Image Thinning with a Cellular Neural Network", *IEEE Transactions on Circuits and Systems*, 37 (5), 638-640, 1990.
- [3]. Sziranyi T. and Csapodi M., "Texture Classification and Segmentation by Cellular Neural Network using Genetic Learning", *Research Report, Computer and Automation Institute Hungarian Academy of Sciences*, Budapest, Hungary, Kasım 1994.
- [4]. Slot K., "Cellular Neural Network Design for Solving Specific Image-Processing Problems", *Internatinal Journal of Circuit Theory and Applications*, 20, 629-637, 1992.
- [5]. Schultz A., "Spatio Temporal CNN Algorithm for Object Segmentation and Object Recognition", *Fifth IEEE International Workshop on Cellular Neural Networks and Their Applications Proceedings*, South Bank University, London, UK, 347-352, 1998.
- [6]. Chua L.O. and Yang L., "Cellular Neural Networks: Theory", *IEEE Transactions on Circuits and Systems*, 35 (10), 1257 - 1272, 1988.
- [7]. Özmen, A., Uçan O.N. ve Albora, A.M., "Arkeolojik Sahalarda Ölçülen Cisimlerin Hücreyel Yapay Sinir Ağları Kullanılarak Görüntülenmesi" *TMMOB Jeofizik Mühendisleri Odası İzmir Şubesi-İZMİR*, 24, 1999.
- [8]. Güzeliş C., "Hücreyel Yapay Sinir Ağları ile Görüntü İşlenmesi", *TÜBİTAK Proje No: EEEAG - 103*, Rapor, İstanbul, 1993.
- [9]. Albora, A. M., Özmen, A. ve Uçan, O. N., "Residual Separation of Magnetic Fields Using a Cellular Neural Network Approach" *Pure and Applied Geophysics*, 158, 1797-1818, 2001.
- [10]. Albora, A. M., Uçan, O.N., Özmen A. and Özkan, T., "Separation of Bouguer anomaly map using cellular neural network" *Journal of Applied Geophysics*, 46, 129-142, 2001.
- [11]. Helvacı, C., "Apatite-Rich iron deposits of the Avnik (Bingöl) Region, Southeastern Turkey" *Economic Geology*, 79, 354-371, 1984.
- [12]. Helvacı, C., and Griffin, W.L., "Metamorphic Feldspathization of Metavolcanics and Granitoids, Avnik Area, Turkey" *Contributions to Mineralogy and Petrology*, 83, 309-319, 1983.

